Available online at www.sciencedirect.com
SCIENCE DIRECT
Polymer 47 (2006) 4683–4693
polymer
www.elsevier.com/locate/polymer

EPR studies of peroxide decomposition, radical formation and reactions relevant to cross-linking and grafting in polyolefins

Susana Camara [a], Bruce C. Gilbert [a,*], Robert J. Meier [b], Martin van Duin [b], Adrian C. Whitwood [a]

[a] Department of Chemistry, University of York, Heslington, York YO10 5DD, UK
[b] DSM Research, P.O. Box 18, 6160 MD Geleen, The Netherlands

Received 10 January 2006; received in revised form 15 February 2006; accepted 4 April 2006
Available online 11 May 2006

Abstract

EPR spectroscopy has been employed to detect directly radicals formed from a variety of polyolefins (PE, PP and EPM) during reaction with peroxide-derived alkoxyl radicals generated by thermolysis. Conditions have been chosen to reflect those employed in polyolefin grafting, degradation and cross-linking. Radical assignment is assisted, in particular, by the recognition of the effects of chirality on the β-proton hyperfine splittings. Quantitative analysis provides information on the selectivity of the initial attack (e.g. methine protons > methylene protons for PP); notable differences in selectivity between alternating EPM and other EPM samples are discussed. The detection of longer-lived allyl radicals detected for PE is explained in terms of alkyl radical disproportionation with subsequent reaction of the product alkene.

Keywords: Free-radical; Selectivity; Polyolefins

1. Introduction

Melt processing of polyolefins in the presence of free-radical initiators has found widespread industrial application [1–3]. For example, free-radical grafting of unsaturated monomers is among the most attractive ways for the chemical modification of polymers such as polyethene (PE); elastomers such as ethene/propene rubber (EPM) and ethene/propene/diene rubber (EPDM) can be readily cross-linked by organic peroxides [3]. Polypropene (PP) can be degraded in a controlled fashion using peroxides [2,4–7]. However, the reaction mechanisms of radical processing are still a matter of debate.

Peroxide cross-linking of polymers, for example, PE, is believed to be achieved via a free-radical mechanism, which involves three key steps: (i) the generation of radicals by thermal decomposition of the peroxide, (ii) radical attack on the polymer chain via hydrogen abstraction to generate polymer radicals and (iii) the combination of two polymer radicals to form carbon–carbon cross-links (see Scheme 1).

Additional reactions may be important: for example, Yamazaki and Seguchi [8,9] have reported EPR studies on the chemical cross-linking mechanism of PE using peroxides at elevated temperatures and have identified both alkyl radicals (1) and allyl radicals (2), the latter, apparently, formed via disproportionation of two polymer radicals and further reaction (see later and also Ref. [10]).

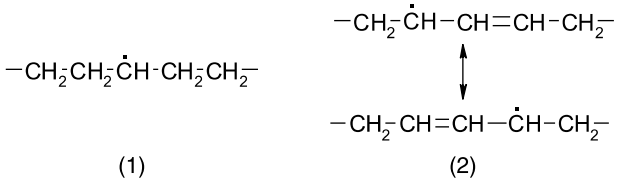

(1) (2)

PP experiences mainly chain scission reactions during peroxide modification, which causes the original molecular weight of the polymer to decrease, though cross-linking of PP can be achieved at high peroxide concentrations [4–7]. Since, combination is a second-order process and fragmentation is a first-order reaction, an increase in the concentration of macroradicals in the reaction mixture leads to a decrease in the proportion of the macroradical fragmentation, resulting in a higher cross-linking efficiency [4]. Other factors, such as the reactivity of the primary radicals derived from the decomposition of the peroxide (and their diffusion rates) and the temperature, are also believed to be important [4]. For example, Zhu and co-workers [11] have proposed that PP

* Corresponding author. Tel.: +44 904 434586; fax: +44 904 432516.
E-mail addresses: suscamara@yahoo.es (S. Camara), bcg1@york.ac.uk (B. C. Gilbert), r.meier@wxs.nl (R.J. Meier), martin.duin-van@dsm.com (M. van Duin), acw1@york.ac.uk (A.C. Whitwood).

0032-3861/$ - see front matter © 2006 Elsevier Ltd. All rights reserved.
doi:10.1016/j.polymer.2006.04.015

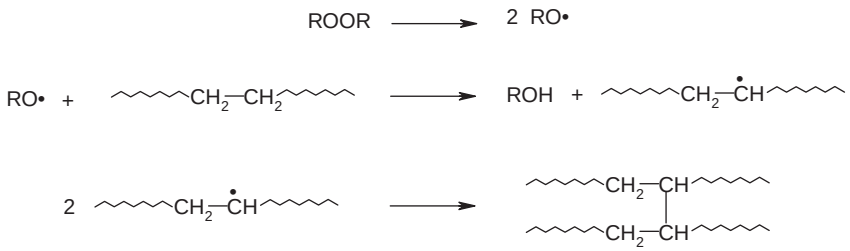

Scheme 1. Cross-linking reaction scheme for PE in the presence of peroxide.

mainly experiences β-scission of tertiary radicals during peroxide modification at high temperature, leading to the formation of a vinylidene group and a secondary radical (see Scheme 2), on the basis of assignment of EPR spectra to a mixture of the tertiary radical (3) and the secondary radicals (4). In contrast, Yamazaki and Seguchi [12] reported that only the tertiary radical (3) is detected under similar conditions.

Many attempts have been made to study the mechanisms involved in the reaction of EPM co-polymers and EPDM ter-polymers with peroxides [12–15], for example, cross-linking and grafting of maleic anhydride [13]. However, the details of these processes, and the effect of the composition of the polymers on cross-linking and grafting are still a matter of speculation.

We have previously employed EPR spectroscopy to study directly the selectivity of hydrogen-atom abstraction by some alkoxyl radicals from a variety of linear and branched alkanes, as well as linear alkenes, chosen as low-molecular-weight models for polyolefins [16]. In situ thermal and photolytic approaches, as well as spin-trapping, provided information relating to a wide temperature range (233–453 K), which mimics the conditions relevant to processing of polyolefins in the melt. The selectivity of hydrogen abstraction was found to be largely governed by enthalpic effects (i.e. tertiary C–H most reactive), but entropy considerations are believed to underlie the relative lack of reactivity of secondary and tertiary C–H bonds in 2,4-dimethylpentane and 2,4,6-trimethylheptane, models for PP (see also Ref. [17]).

The main aim of the work to be described here was to extend our previous study to high-molecular-weight polymer systems and to explore the selectivity of radical formation and reaction of polyolefin chains in the presence of oxygen-centred radicals. Our approach has employed thermal conditions involving temperatures over 430 K, similar to those used for polyolefin processing in the melt.

Experiments involved an extension of the in situ high-resolution EPR spectroscopic studies, using decomposition of dicumyl peroxide (5) (DCP) and 2,5-bis-(*tert*-butylperoxy)-2,5-dimethylhexane (6) (BPDH) to generate alkoxyl radicals under steady state conditions. In situ thermolysis experiments, involving the decomposition of peroxides in the presence of a variety of polyolefins, including PE wax, high density PE (HDPE), PP with different tacticity (isotactic, syndiotactic and atactic) and a variety of random EPM co-polymers with % (w/w) propene varying from 22 to 95%. This approach has allowed us to obtain relative rates of attack of alkoxyl radicals on C–H bonds in a range of different polyolefins. EPR spectroscopy allows us to distinguish between radicals derived from different sequences of monomers, the recognition of the importance of the effect of chirality being vital in the interpretation of results. Factors governing the selectivity of reaction, such as the peroxide concentration and the distribution of the CH and CH_2 groups along the polymer chain are reported. Other approaches including kinetic modelling have been employed in order to support mechanistic interpretations.

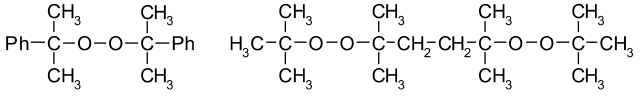

(5) (6)

2. Experimental

2.1. Sample preparation

For some experiments, the peroxide was incorporated into the sample by mixing in a 50 cc Brabender batch mixer. A second procedure, melt-mixing in a stirred vessel, was exclusively applied to the sample of low-molecular-weight

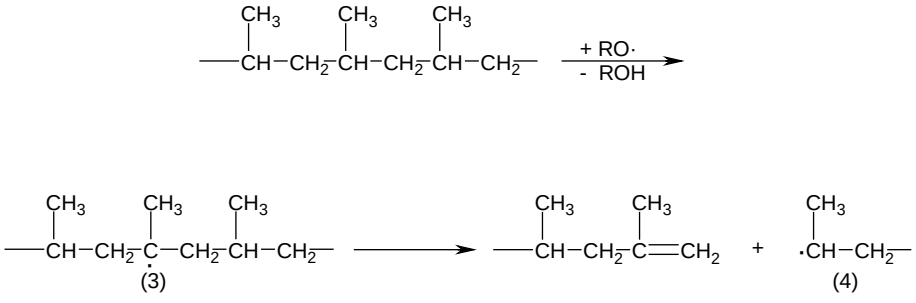

Scheme 2. Proposed mechanism for the β-scission of tertiary radicals in PP.[11]

PE wax. Because of the low melting point of the wax (~60 °C), the peroxide could be mixed in by melting the wax at temperatures at which the peroxide would not yet show any detectable decomposition. In other experiments, polymer samples had peroxide incorporated by a solvent-based procedure, which involved dissolving the polymer in a refluxing solvent (e.g. hexane or xylene), cooling the mix to room temperature, addition of the peroxide and finally removal of the solvent by evaporation at ambient temperature and pressure.

The peroxides, DCP (5) and BPDH (6) were obtained from Aldrich. The half-lives of the peroxides were calculated from their reported activation parameters; for example, at 443 K the calculated half lives are 99 s for (5) and 117 s for (6) [18]. The PE, PP, and EPM samples were provided by DSM.

2.2. EPR spectroscopy

Polymer samples containing peroxides were typically heated to ca. 443 K in the cavity of the EPR spectrometer, in order to produce a flux of oxygen-centred radicals for reaction with the polymers. Spectra of the resulting substrate-derived radicals were typically recorded via repeated rapid scans starting almost immediately (ca. 40 s) after insertion of the sample and continued over a period of ca. 12 min.

EPR spectra were recorded on a Bruker ESP300 EPR spectrometer equipped with an X-band microwave bridge and TE102 cavity. Temperature control was achieved using a Bruker ER-4111 variable-temperature controller, calibrated using an independently calibrated thermocouple. The polymer substrate mixed with the peroxide was placed in a borosilicate sample tube (o.d. 5.0 mm). The EPR cavity was pre-heated to the required temperature (typically 453 K) and once achieved, the sample was placed in the cavity. The sample subsequently reached the required temperature within 50 s; the heating profile of a sample placed in the pre-heated cavity had been determined previously using a separate thermocouple placed in a sample tube filled with eicosane. A number of spectra were then recorded, typically with a scan time of 40 s, modulation amplitude 0.16 mT, microwave frequency ~9.35 GHz and microwave power 10 mW. Absolute radical concentrations were determined by comparison of the double integrals of experimental EPR spectra with that of a standard weak pitch sample under identical spectrometer conditions. The pitch sample was calibrated by comparison, at room temperature, with the spectrum obtained from a solution of the stable nitroxide 4-hydroxy-2,2,6,6-tetramethylpiperidine-1-oxyl (TEMPOL) with a known concentration. Direct comparison of the TEMPOL and experimental spectra at high temperatures was not possible, because of thermal degradation of TEMPOL.

Isotropic spectra were simulated using a program, which allows the simulation of up to ten different radical species and allows variation in g-values, splittings (a_H), concentrations and line-widths as well as the incorporation of second-order effects. The computer program, WinEPR (Bruker Spectroscopy), was used to convert the output from the EPR spectrometer into a suitable format for manipulation, especially baseline correction. Kinetic simulations were performed using the Simula program originally written by Dr T.M.F. Salmon and kindly provided by Shell Global Solutions PLC.

2.3. GC–MS studies of model compounds

DCP [(5), 1–10 wt%] was dissolved in decane, in alkenes (1-octene, 4-octene) or decane/alkene mixtures (10:1; w/w). These solutions were heated for 30 min at 433 K in a nitrogen atmosphere. Subsequently, samples were analysed using gas chromatography (HP 6890 GC with a 30 m long, 0.25 mm internal diameter, CP SIL 8 CB column; temperature programmed from 30 to 255 °C) with mass spectrometry detection (HP 5973 MSD).

3. Results and discussion

3.1. Polyethene

3.1.1. EPR spectra of radicals detected from low-molecular-weight PE wax

Initial thermolysis experiments were performed with PE wax, chosen to bridge the gap between the studies of low-molecular-weight hydrocarbons such as eicosane ($C_{20}H_{42}$) and tetracontane ($C_{40}H_{82}$), studied previously [16], and the high-molecular-weight polymers (see later). Experiments involved thermolysis of a mixture of the polymer and the peroxide in the EPR cavity. Thermolysis (443 K) of samples of the polymer, mixed with DCP (5) at a concentration range of 2–8% via dissolution (see Section 2) or 2% using a batch mixer or 10% w/w melt-mixed with the wax, gave rise to (weak) EPR signals with hyperfine splittings a_H 2.12, a_{H4} 2.40 mT and g 2.0026, assigned to the alkyl radical (1) formed by hydrogen-abstraction from the PE backbone; no other radicals, e.g. the allyl radical (2), were observed. The optimum EPR signals were obtained at 443 K, at other temperatures (both higher and lower) either weak signals or no signals were observed.

In further experiments with the PE wax and BPDH (6), it was found that both melt-mixing and solvent mixing (peroxide concentration from 6 to 30% w/w) led to the detection of the alkyl radical (1). The observation of only alkyl radicals for samples with the peroxide mixed with the substrate is fully consistent with the results obtained previously [16] for eicosane (predominantly secondary alkyl radicals) and tetracontane (only secondary alkyl radicals).

On the other hand, experiments, which involved simply pouring the peroxide, BPDH (6), onto the wax (30% w/w) without any mixing, revealed both alkyl (1) and also a second radical with hyperfine splittings a_H 0.44, a_{6H} 1.37 mT and g 2.0026, characteristic [8] of the allyl radical (2) (similar to those observed for HDPE, see Fig. 1). Initially, only the spectrum from the alkyl radical was observed, but with time the intensity of the alkyl radical signals decreased, whereas the signals arising from the allyl radical (2) appeared and increased (see below). At lower peroxide concentrations, e.g. 10% w/w of either (5) or (6), no allyl radicals were observed. These observations suggest that high local peroxide concentrations,

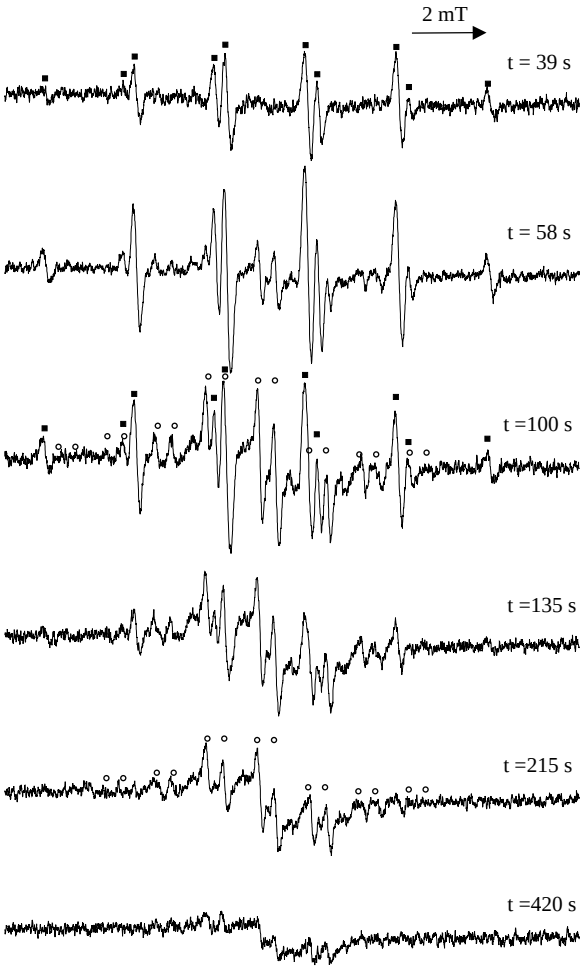

Fig. 1. ESR spectra of HDPE/30% w/w BPDH (6) recorded at different stages of the reaction at ca. 443 K, showing signals from the alkyl radical (1, ■) and allyl radical (2, O); *t* is the time after mixing that the scan was started.

due to inhomogeneous mixing, induce the formation of allyl radicals (see later).

3.1.2. EPR spectra of radicals detected from HDPE

Experiments with HDPE and 30% BPDH (6), mixed using the dissolution method, gave rise initially to considerably stronger signals of the alkyl radical (1) and also to signals from the allyl radicals (2) (Fig. 1). The alkyl signal first increased, and then decreased as a function of time (see Fig. 2). A maximum alkyl radical concentration of ca. 4×10^{-6} mol dm^{-3} was achieved after ca. 80 s and a maximum allyl radical concentration of ca. 1.7×10^{-6} mol dm^{-3} after ca. 400 s. Experiments with a range of peroxide concentrations revealed that more intense signals were observed at higher peroxide concentrations and that a minimum peroxide concentration of 15% was required to obtain signals. Similar behaviour was noted with DCP (5). It was notable that in these experiments total peroxide dissolution was not achieved and it is therefore unlikely that the peroxide is homogeneously distributed.

In order to establish whether or not the allyl radicals detected derive from unsaturation already present in the polymer, three HDPE samples containing different types

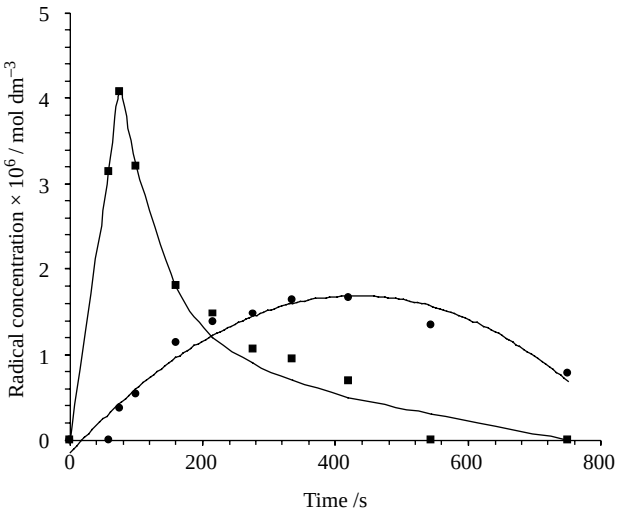

Fig. 2. Variation in concentration of alkyl (1, ■) and allyl (2, ●) radicals detected by EPR with time for a sample of HDPE containing 30% w/w of peroxide (6) at 443 K.

Table 1
Number of alkene groups (per 10^5 carbons) in HDPE samples prior to thermolysis as determined by FT-IR spectroscopy

Sample	Terminal	trans	Pendant vinyl
1	1	7	2
2	4	2	23
3	19	5	28

NB. Identical EPR spectra were obtained from all samples, see text.

(and amounts) of alkenes groups (terminal, trans and pendant, see Table 1) were studied. Identical EPR signals were obtained from all samples, attributed to alkyl and allyl radicals (with hyperfine splittings as above, see Fig. 1). No signals were obtained, which could be attributed to (allyl) radicals from terminal alkenes or pendant vinyl alkenes already present. Thus, the allyl radicals directly detected for PE are derived from unsaturation formed upon reaction with peroxide, rather than those initially present.

3.1.3. IR studies of unsaturation in PE samples

To investigate further why allyl radicals are detected in the HDPE-derived EPR spectra (in contrast to the behaviour of PE wax and the model compounds, eicosane and tetracontane [16]), the PE/peroxide mixtures, which had been studied by EPR at 443 K were quantitatively analysed for alkene content by FT-IR spectroscopy. These samples contained different concentrations of peroxide (6) (10, 20 and 30% w/w) in which a solvent mixing-procedure was used to incorporate the peroxide in the samples; a peroxide-free HDPE sample was also analysed for comparison. The IR data allowed quantification of the bands at 908 cm^{-1} for terminal unsaturation and 965 cm^{-1} for *trans* unsaturation in each sample (see Table 2).

The IR data show a significant decrease in terminal unsaturation and a slight increase of trans unsaturation with increase of peroxide concentration in the sample. The extent of

Table 2
Number of alkene groups (per 10^5 carbons) in samples of HDPE and peroxide (6) thermolysed for ca. 12 min at 443 K as determined by FT-IR spectroscopy

% Peroxide (w/w)	trans	Terminal
0	3	115
10	8	28
20	11	9
30	14	9

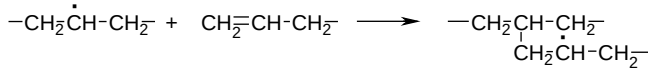

Scheme 3. Addition of secondary alkyl radical to terminal unsaturation of PE.

unsaturation formed after the thermolysis process is broadly similar to the extent of unsaturation in the samples described previously (Table 1).

The decrease in terminal unsaturation is consistent with the predominant addition of secondary macroradicals formed in the PE chain onto the terminal alkene (see Scheme 3) as a result of the more rapid attack on terminal alkenes compared to mid-chain double bonds (cf. Refs. [19,20]).

The increase of trans unsaturation observed would be consistent with the occurrence of a disproportionation reaction (see Scheme 4 and later), which is second-order in radical concentration and thus strongly favoured by high local concentrations of peroxide in the sample (due to inhomogeneous mixing of the peroxide within the polymer) and hence the high local radical concentrations. The observation that the formation of trans unsaturation is clearly dependent on the peroxide concentration is in agreement with the findings of Smedberg et al. [21] and is in contradiction with the mechanism proposed by Bremner [20], which implies the conversion of terminal into trans unsaturation.

3.1.4. GC–MS analysis of reaction products from model compounds

GC–MS results obtained from a set of model experiments provide support for the occurrence of dimerization and disproportionation reactions and the radical addition reaction shown in Scheme 3 (see Table 3). They involved the decomposition of DCP (5) in the presence of low-molecular-weight hydrocarbons at high temperature (ca. 433 K). For decane, saturated dimers were mainly formed, as a result of decyl radical combination, together with a smaller amount of unsaturated products (i.e. decenes). For 1-octene and 3-octene, mainly dimers were formed as a result of allyl radical combination. For 1-octene, some mono-alkene dimers were formed by addition of the allyl radical onto the double bond of 1-octene. When mixtures of decane and 1-octene were studied (in a volume ratio 10:1), saturated products were obtained as a result, presumably, of the addition reaction of alkyl radicals to the terminal double bound. For a mixture of decane and 3-octene (an alkene with internal unsaturation) both mono and di-unsaturated products, but no saturated products, were identified indicating that combination of radicals has occurred rather than radical addition to the double bond.

3.1.5. Kinetic modelling of allyl radical formation

Our initial aim was to develop a prototype kinetic model, which simulates the concentration profiles of alkyl and allyl radicals observed during the thermolysis at ca. 443 K of HDPE/30% w/w BPDH (6) (Fig. 2) and accounts, in particular, for the formation and apparent longevity of the allyl species.

The initial model (see Scheme 5) incorporates reactions (1)–(7), which involve decomposition of the peroxide [reaction (I)] to generate alkoxyl radicals, hydrogen abstraction from the polymer chain by alkoxyl radicals to give alkyl ($P^{\bullet}$) radicals [reaction (II)]. Termination reactions included combination of two alkyl, two allyl, or one alkyl and one allyl radical, [reactions (III), (VI) and (VII), respectively], all of which give cross-linking. We propose that the allyl radical arises from radical attack upon an alkene [reaction (V)], itself formed via an additional termination reaction, i.e. disproportionation of two alkyl radicals [reaction (IV)] as described earlier.

The concentration of CH_2 groups in HDPE was taken as 44.64 mol dm^{-3} and for the peroxide 0.94 mol dm^{-3} [to mimic the experimental conditions of a sample of HDPE with a density of 0.9 g cm^{-3} and 30% w/w of BPDH (6)]. The rate constant for the decomposition of the peroxide [reaction (I), k 7.7×10^{-3} s^{-1}] was calculated taking into account the values of A (Arrhenius frequency), E_a (activation energy) [18] and a temperature of 443 K. Predicted values of A and E_a for the abstraction reactions (II) and (V) were obtained from a compilation by Howard et al. [22] from which rate constants for these reactions were calculated as 1.6×10^6 and 1.0×10^7 dm^3 mol^{-1} s^{-1}, respectively. Rate constants and concentrations have been expressed on a per CH_2 basis.

The rate constants for reactions (III), (IV), (VI) and (VII) were then varied systematically over limited but realistic ranges and the effects on the predicted radical concentrations was studied. Most of the calculations clearly failed to reproduce the growth of the allyl concentration and, in particular, its delayed appearance. However, for certain combinations of rate constants, it is possible to obtain reasonable agreement between observed and predicted profiles of both the alkyl and allyl radicals. These sets of calculations had two major characteristics: firstly, a very low rate of termination of allyl radicals (e.g. k_{VI} ca. 5×10^3 dm^3 mol^{-1} s^{-1}) and, secondly, a ratio of the rate constants for combination to disproportionation for the alkyl radicals of k_{III}:k_{IV} ca. 10^5:1. The former feature is believed to largely reflect an (observed) prolonged lifetime of the allyl radicals (and hence their detection), which itself may be related to the increasing viscosity of the polymer matrix. The second feature reflects a (predicted) relatively slow build-up of alkene

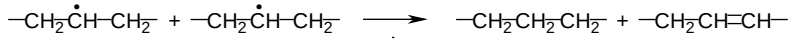

Scheme 4. Disproportionation of secondary radicals.

Table 3
Examples of dimeric and related structures identified by GC–MS analysis upon thermal decomposition (at ca. 433 K) of peroxide (30% w/w DCP) in low-molecular-weight substrates

Substrate	Product[a]	
	Major	Minor
Decane ($C_{10}H_{22}$)	$C_{20}H_{42}$ dimers, e.g. 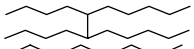	Decenes ($C_{10}H_{20}$), e.g. 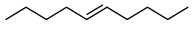
1-Octene (C_8H_{16})	$C_{16}H_{30}$ dimers, e.g. 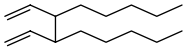	$C_{16}H_{32}$ dimers, e.g. 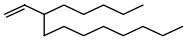
3-Octene (C_8H_{16})	$C_{16}H_{30}$ dimers, e.g. 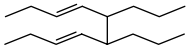	–
Decane/1-octene (10:1 v/v)	$C_{18}H_{38}$, e.g. 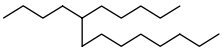	–
Decane/3-octene (10:1 v/v)	(a) $C_{16}H_{30}$ dimers, e.g. 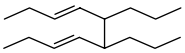	–
	(b) $C_{18}H_{36}$, e.g. 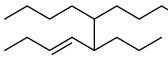	

[a] The precise structure of the dimers was not determined.

and hence delayed appearance of the allyl radical. Because of the build-up of alkene, we introduced an extra reaction through which allyl radicals arise from the reaction of alkyl radicals with the alkene (reaction VIII). A value of 10^3 dm^3 mol^{-1} s^{-1} led to a noticeable increase in the calculated concentration of the allyl radical.

$$\text{P(alkene)} + \text{P}\cdot \rightarrow \text{P(allyl)}\cdot + \text{PH} \qquad \text{(VIII)}$$

Fig. 3 shows the best calculated fit based on the rate constants given above (reactions I–VIII). Clearly, these calculations only represent a simplistic approach to a complex set of reactions, occurring in a medium in which viscosity is steadily changing, and the system does not take into account the time taken for the sample to reach 453 K after insertion into the EPR cavity. Nevertheless, the results appear to offer support to the conclusion that, as identified in the scheme, the observed allyl radicals derive from hydrogen abstraction from alkenes, which build-up via disproportionation of the initial alkyl radicals.

3.2. Polypropene

A variety of PP samples, including those with different tacticity (isotactic, syndiotactic and atactic) were next explored.

The EPR spectrum recorded using samples of isotactic PP (*i*-PP) with 8% w/w of DCP (5) at 433 K showed signals derived exclusively from the tertiary radical (3), with hyperfine splittings a_{3H} 2.27, a_{2H} 1.97 and a_{2H} 1.56 mT with *g*-value 2.0026, characterised by the non-equivalence of the β-protons (see below, cf. Ref [12]). The sequence of EPR spectra recorded over time (ca. 4 min) showed a progressive decay in the intensity of the signals. No other signals were observed. BPDH (6) was also used as the initiator, in concentrations up to 30% w/w, and similar results, with slightly enhanced resolution and intensity were obtained. Signals derived from (3) were also obtained with *s*-PP and *a*-PP samples but with a decrease in the intensity of the signals from *i*-PP to *s*-PP to *a*-PP. This may reflect a decrease in the viscosity and hence an increase in the rate constant for termination.

A key observation is the non-equivalence of the β-proton splittings that reflects the presence of a chiral carbon (in the γ-position) [23], though restricted rotation (hindered motion of the polymer) may also contribute [24]. Lack of line-width variation (across the spectrum and as a function of temperature) strongly suggests that the non-equivalence reflects the chirality of the γ-carbon under these conditions. Analysis of a(β-H) values employing the expected angular dependence [16] of β-proton splittings [$a(\beta\text{-H}) = \rho_\sigma B \cos^2\theta$] suggests that the appropriate average dihedral angles (θ) between the non-equivalent β-protons and the p-orbital of the unpaired electron are ca. 49.5 and 53.9°. There were no detectable signals from the secondary radical (7); which is in agreement with the absence of secondary radicals in experiments using 2,4-dimethylpentane and 2,4,6-trimethylheptane (models for PP) [16]. This observation may be explained by particularly high transition-state energy barriers, which reflect unfavourable entropies of activation, as suggested by DFT calculations [16].

				Rate constant		Ref
ROOR	→	RO· + RO·	(I)	7.7×10^{3} s^{-1}		[18]
RO· + PH	→	ROH + P·	(II)	1.6×10^{6} dm^3 mol^{-1} s^{-1}		[22]
P· + P·	→	P–P	(III)	varied		
P· + P·	→	PH + P(alkene)	(IV)	varied		
RO· + P(alkene)	→	ROH + P(allyl)·	(V)	1.0×10^{7} dm^3 mol^{-1} s^{-1}		[22]
P(allyl)· + P(allyl)·	→	P(allyl)–P(allyl)	(VI)	varied		
P(allyl)· + P·	→	P(allyl)–P	(VII)	varied		

Scheme 5.

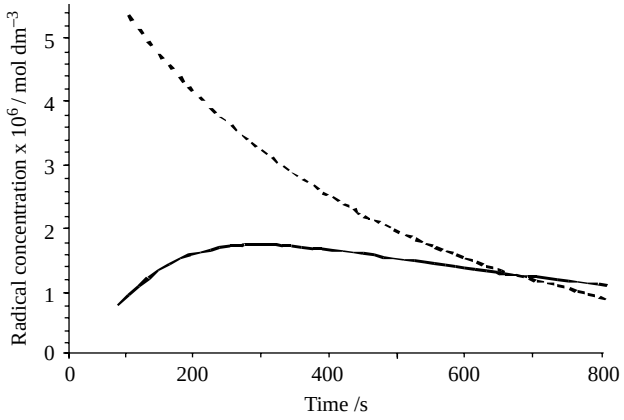

Fig. 3. Variation of simulated radical concentration with time for alkyl (dotted line) and allyl (solid line) radicals; see text for details.

The absence of the primary radical (8) may reflect its lack of formation or the occurrence of rapid (1,6) intra-molecular hydrogen-transfer from a primary to a more stable tertiary radical. It is particularly notable that no signals were observed from (4), claimed by Zhu and co-workers [11] to be formed by β-scission. This is not surprising: if we employ values of A ($10^{14.1}$) and E_a (134 kJ mol^{-1}) reported for β-scission of C–C bonds in small molecules the rate constant is calculated to be ca. 7×10^{-3} s^{-1} at 433 K [6], i.e. far too slow to give a detectable signal under these conditions.

These results, obtained at very high peroxide concentration, evidently reflect conditions, which lead to a high concentration of tertiary alkyl radicals. Therefore, under these conditions, cross-linking will be favoured over fragmentation, which would be expected to cause a lowering of the molecular weight of the polymer, expected at low peroxide concentration (usually <1 wt%) [4,6].

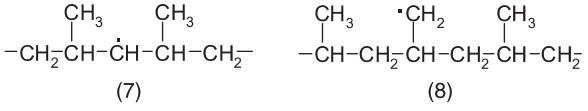

3.3. Ethene/propene co-polymers (EPM)

A series of EPM co-polymers was next studied in which the concentration of propene ranged from 22 to 95% (w/w). We note that in EPM co-polymers with propene levels up to ca. 60% (w/w) there is a strong tendency towards isolated propene units (i.e. –EPE– sequences dominate) because the Ziegler-Natta catalysts do not favour propene propagation. In addition, a sample of alternating EPM, prepared by hydrogenation of natural rubber, was also studied. In all cases, experiments involved mixture with DCP (5) (10% w/w) and thermolysis at ca. 443 K.

3.3.1. EPM with 22 and 27% w/w of propene

Complex EPR patterns were obtained, which are believed, on the basis of detailed spectrum simulation and the changes of signal intensities over time, to be composed at least of four radicals (see Fig. 4); one of which is more clearly seen after

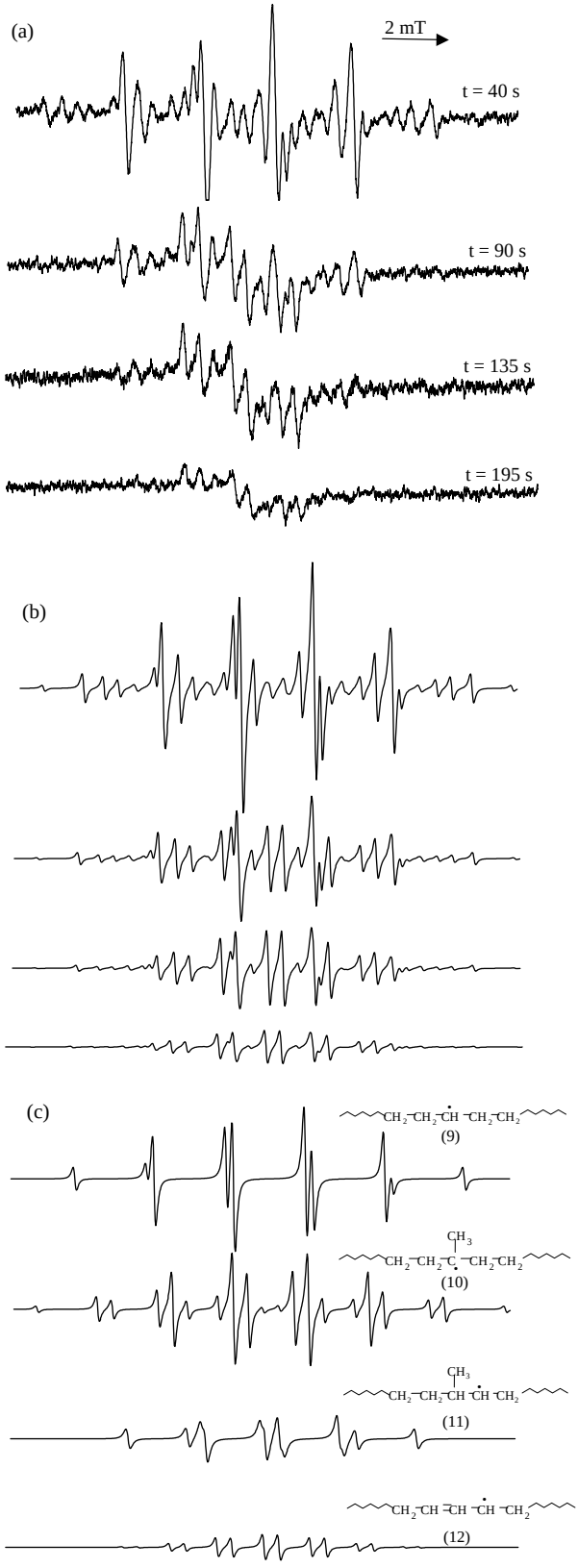

Fig. 4. EPR spectra of a mixture of radicals (9), (10), (11) and (12) obtained with a sample of EPM (22% w/w propene) containing 30% w/w of BPDH (6) at 443 K. t is the time after mixing that the scan was started. (a) Experimental spectra; (b) simulation of spectra based on hyperfine splittings (see Table 4) and proportions (see Fig. 5); (c) individual components, which contribute to the simulations shown in (b).

Table 4
Hyperfine splittings for radicals detected in EPM co-polymers together with predicted ethene/propene sequences along the co-polymer chain based on the radical observed

Radical	Splitting constants (mT)[a]		Sequence of ethene/propene
	α	β	
(9)	2.16 (1H)	2.38 (4H)	–EEE–
(10)	–	2.27 (3H)	–EPE–
		1.82 (4H)	
(11)	2.18 (1H)	1.77 (1H)	–EPE–
		2.30 (2H)	
(12)	0.44 (1H)		
	1.37 (2H)	1.37 (4H)	–EEE–
(13)	–	2.27 (3H)	–PPP–
		1.97 (2H)	
		1.56 (2H)	
(15)	–	2.27 (3H)	–EPE–
		1.82(4H)	
(16)	2.16 (1H)	2.38 (2H)	–PEP–
		2.30 (2H)	
(17)	2.18 (1H)	1.92 (1H)	–PEP–
		2.34 (2H)	

[a] Estimated as ca. ±0.005.

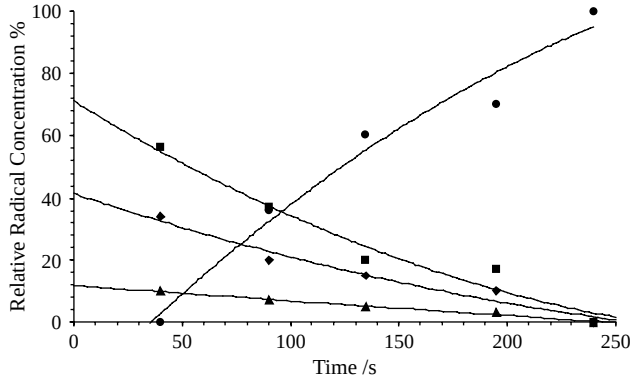

Fig. 5. Variation of relative concentration as a function of time for radicals (9, ■), (10, ♦), (11, ▲) and (12, ●) detected in the EPR spectra obtained with a sample of EPM (22% propene) w/w containing 30% w/w of BPDH (6) at 443 K.

a period of time. In the first spectrum (recorded after 40 s) signals from three radicals can be clearly characterised. The dominant pattern is a doublet of quintets with hyperfine splittings a_H 2.16 and a_{4H} 2.38 mT and g-value 2.0026, assigned to the mid-chain polyethene-type radical (9) (see Table 4). The expected tertiary radical (10), derived from a propene monomer located between two ethene monomers (i.e. EPE) can also be identified with hyperfine splittings a_{4H} 1.82 and a_{3H} 2.27 mT and g-value 2.0026. The third radical has a_H 2.18 (assigned to an α proton), $a_{\beta\text{-}1H}$ 1.77 and a_{2H} 2.30 mT and g-value 2.0026 consistent with abstraction of a hydrogen from a methylene group next to a methine group to give a secondary radical [see (11)], again due to EPE sequences. The assignments to (10) and (11) are based on the equivalence of the β-protons observed in these species, which indicates the presence of a non-chiral carbon in the γ-position and, hence, implies the presence of ethene moieties adjacent to the propene monomer. The initial relative concentrations (expressed as a percentage) for radicals (9), (10) and (11) are 56, 34 and 10%, respectively (see Fig. 5).

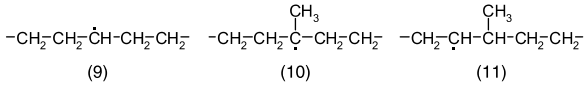

The EPR spectra recorded after 90 s showed additional signals typical of an allyl radical [assigned the structure (12)], with a_H 0.44 and a_{6H} 1.37 mT and g-value 2.0026. The EPR spectra recorded showed an increase of the allyl radical concentration over time, whilst the intensity of the signals derived form the alkyl radicals gradually decreased. Similar results were obtained with EPM-27% w/w propene, although the concentration of the tertiary radical is somewhat higher, which reflects the higher contribution of propene in the composition of the co-polymer (Table 5).

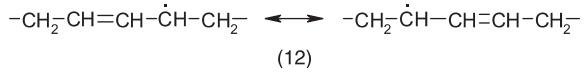

3.3.2. EPM with 55% w/w of propene

Complex EPR patterns similar to those obtained with EPM containing 22 and 27% propene were observed, although important differences are notable (see Fig. 6). Again, at least four radicals were detected. The sharp doublet of quintets, with a_H 2.16, a_{4H} 2.38 mT and g-value 2.0026, assigned to the mid-chain PE type radical (9), is less dominant as might be anticipated because of the higher propene content. The

Table 5
Relative concentration (%) as a function of time for radicals (9)–(12) derived from EPM-22% w/w propene, observed during its reaction with DCP (10% w/w) at ca. 443 K

Radical	Ratio (%)[a]				
	40 s	90 s	135 s	195 s	240 s
(9)	56	37	20	17	0
(10)	34	20	15	10	0
(11)	10	7	5	3	0
(12)	0	36	60	70	100

[a] Estimated as ca. ±2.5.

dominant pattern derives from the tertiary radical (10), with a_{4H} 1.82 and a_{3H} 2.27 mT and g-value 2.0026. The equivalence of the β-protons again suggests that this signal derives from a propene monomer between two ethene units (i.e. a part structure –EPE–). The third radical is a secondary radical with an adjacent methine group (11) with $a_{\alpha\text{-H}}$ 2.18, $a_{\beta\text{-1H}}$ 1.77 and a_{2H} 2.30 mT and g-value 2.0026. The relative concentrations of radicals (9), (10) and (11) in this case were 30, 55 and 15%, respectively, in the first spectrum recorded (after 40 s). A gradual decrease for all peaks was observed. Additional signals derived from an allyl radical (a_H 0.44 and a_{6H} 1.37 mT and g-value 2.0026), attributed to radical (12) developed with time. The signals from this species are difficult to observe in the final stages of the reaction, in contrast to results described for the EPM polymers with lower concentrations of propene (see above).

No signals were observed which could be attributed to the tertiary radicals (13) or (14) (derived from –PPP– and –EPP– sequences) where the presence of one or more γ-chiral centres would be expected to cause inequivalence of the β-protons (see below). This may reflect the relatively low concentration of PP pairs (see above) and/or a relatively low reactivity of tertiary hydrogens in propene sequences. A similar low reactivity has been observed for the tertiary position in 2,4-dimethylpentane compared to the tertiary positions in 3-methylpentane and 4-methylheptane [16].

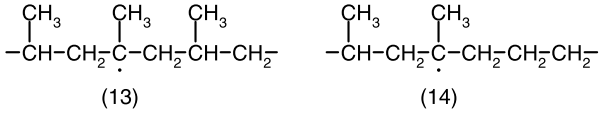

(13) (14)

3.3.3. Alternating EPM (60% w/w of propene)

The EPR obtained from alternating EPM (Fig. 7) is markedly different from that obtained with EPM-55% propene described above although the ethene to propene ratio is approximately the same. The dominant signals are assigned to the tertiary radical (15) with hyperfine splittings a_{3H} 2.27 mT and a_{4H} 1.82 mT (i.e. with equivalent β-protons), g-value 2.0026. A second radical has hyperfine splittings a_H 2.16 mT, a_{2H} 2.38 and a_{2H} 2.30 mT, g-value 2.0026, and is assigned to (16) formed by the abstraction of a hydrogen from the central methylene group; the non-equivalence of the β-protons reflects the chirality of the γ-carbons. Similar results were obtained for the model compound, squalane [16]. The secondary radical (17) was also observed with $a_{\alpha\text{-H}}$ 2.18, $a_{\beta\text{-1H}}$ 1.92 and a_{2H} 2.34 mT,

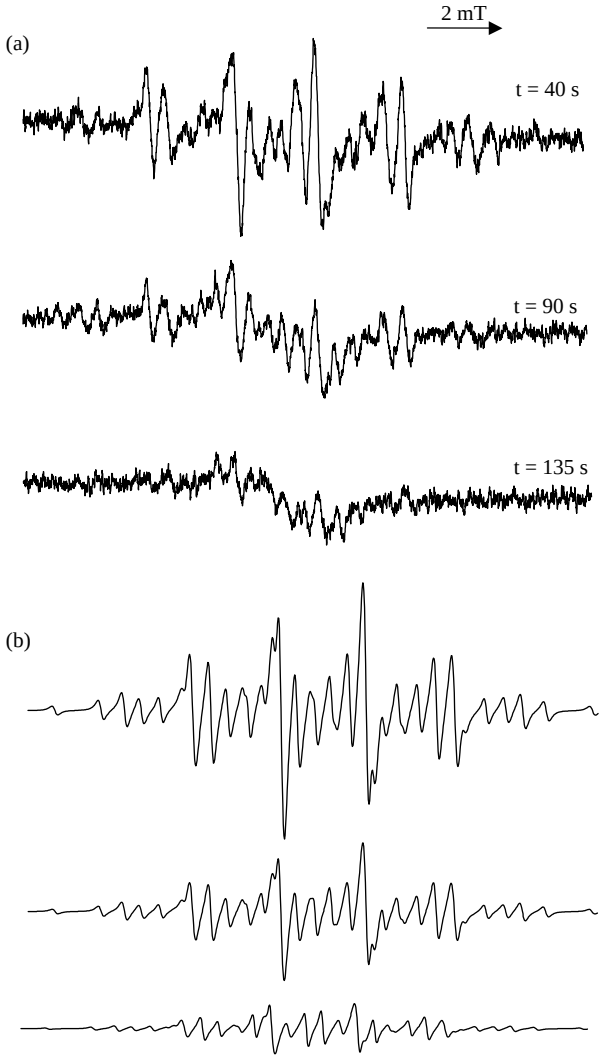

Fig. 6. EPR spectra obtained with a sample of EPM (55% w/w propene) containing 30% w/w of peroxide (6) at 443 K; t is the time after mixing that the scan was started. (a) Experimental spectra; (b) simulation of spectra based on hyperfine splittings (see Table 4).

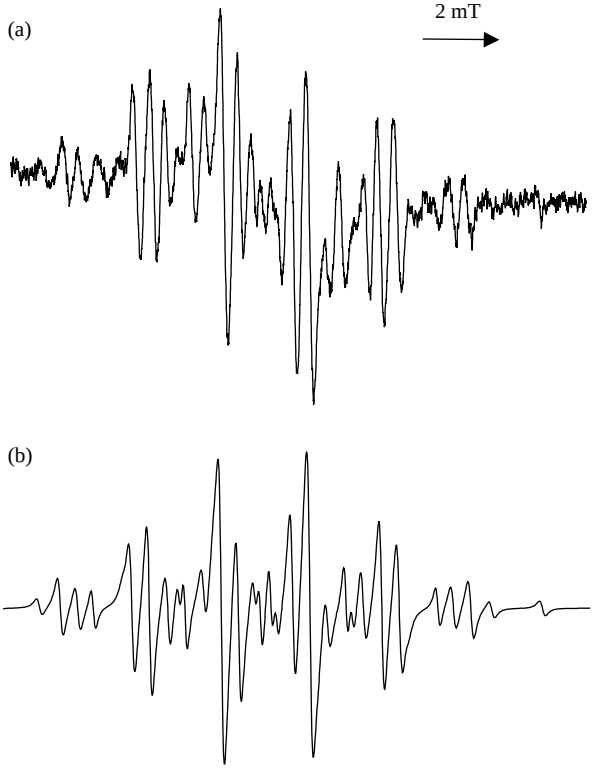

Fig. 7. EPR spectra obtained with a sample of alternating EPM containing 30% w/w of peroxide (6) at 443 K. (a) Experimental spectra of (15), (16) and (17); (b) simulation of spectra based on hyperfine splittings and proportions in the text.

g-value 2.0026. Relative concentrations of (15), (16) and (17) at the start of the experiment were 67, 20 and 13%, respectively. No allyl radicals were detected. These results are broadly comparable with those obtained from squalane under thermolytic conditions (where relative concentrations of 65 and 35% for tertiary and secondary alkyl radicals, respectively). The relatively low selectivity for radical (17) via attack on a methylene next to a methine group has also been observed in the model compound 4-methylheptane. A similar selectivity for methine positions has been observed for the grafting of maleic anhydride onto alternating EPM polymers [13].

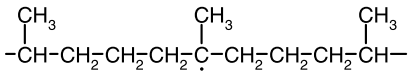

(15)

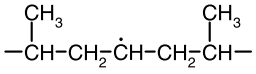

(16)

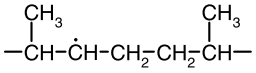

(17)

3.3.4. EPM with 74 and 95% w/w of propene

The initial EPR spectrum from EPM-74% (after 40 s) was simulated with a combination of a tertiary radical (13), with hyperfine splittings a_{3H} 2.27, a_{2H} 1.97 and a_{2H} 1.56 mT, *g*-value 2.0026, derived from sequences of propene monomers, as reflected in the non-equivalence of the β-protons and the mid-chain –EEE– type radical (9) with hyperfine splittings a_{1H} 2.16, a_{4H} 2.38 mT, *g*-value 2.0026; the relative concentrations were 86 and 14%, respectively. No allyl radical signals were observed.

The EPR spectrum for EPM-95% w/w propene was identical to that obtained for PP, i.e. only the tertiary radical (13) was observed. No signals from (14) were obtained.

4. Conclusions

The EPR results described here allow us to draw conclusions firstly about the selectivity of attack on C–H bonds (tertiary, secondary, primary) in different environments (in PP and EPM) and secondly about the mechanism and the relative ease of formation of allyl radicals (in PE and EPM). We note that in industrial processes for polyolefin cross-linking, degradation and grafting, peroxide levels are typically less than 5% w/w. The levels used here (10–30%) were employed to allow a sufficient rate of radical generation to allow direct detection by EPR. However, the ratio of radicals observed is still believed to reflect directly the points of attack of the polymer chains.

The exclusive detection of tertiary radicals (3) in the reaction of alkoxyl radicals with PP at ca. 440 K is entirely consistent with expectations based on enthalpic effects (BDE $CH < CH_2 < CH_3$) and the results of both DFT calculations and EPR observations on model compounds including 2,3-dimethylpentane [16]. Whilst primary radicals (e.g. $\cdot CH_2CHMeCH_2CHMe_2$) are also detectable for the models, this presumably reflects the higher number of methyl CH bonds in these compounds. Failure to detect the corresponding radical from secondary hydrogen abstraction for PP (as with the model compound) evidently reflects the lack of reactivity of these (CH_2) bonds, attributed to steric hindrance and entropy effects in the transition-state [16,17].

The results for the alternating EPM (1:1) co-polymer are also instructive. The values of 67% [for (15)], 20% [for (16)] and 13% [for (17)] give relative rates of attack, on a per-hydrogen basis, of 21:3:1, respectively, for tertiary, secondary ($CH_2\dot{C}HCH_2$) and secondary adjacent to the tertiary carbon ($\dot{C}HCHMe$), with a ratio of 1:7 for CH_2 (central methylene) to CH. We believe that these figures represent relatively unhindered methine and methylene groups, though the reduced value for the methylene next to the tertiary carbon is significant (cf. the behaviour of the model compound squalane) [16] The dominant attack on the methine C–H bonds is consistent with conclusions based on the ^{13}C NMR study of the grafting of maleic anhydride onto EPM [13].

The result for EPM with relatively low propene content (22% w/w propene, i.e. 84 mol% ethene, 16 mol% propene), which gives 34% of the tertiary radical (10) and 56% of the secondary radical (9) as well as 10% of the secondary radical (11) allows us to calculate a ratio of 13.6:1.2:1, respectively, for the per-hydrogen rates of attack [with a ratio of ca. 11:1 for tertiary (EPE) to secondary (EEE)]. The difference between this value and that noted above for the alternating co-polymer may reflect the lower steric hindrance in this case (i.e. for relatively isolated propene units).

For EPM with a concentration of 55% propene (w/w) (50% of –EPE– radicals and 30% of –EEE– structures) the results can be interpreted on a similar basis. The lack of observation of radicals derived from –PPP– sequences is as expected (see above). For high propene-content EPM (74% propene w/w) the observation of radicals derived from –EEE– and –PPP– sequences suggests that this polymer contains a significant proportion of PE and PP type segments.

Fig. 8 provides a summary of the selectivity of H-abstraction from methylene, rather than methine, units for the whole series of polyolefins from PP (50% CH_2 in the polymer backbone) via EPM to PE (100% CH_2). A reasonable correlation exists, showing a monotonic increase in formation of secondary radicals with methylene content.

It is also of interest to compare our findings with the results of a detailed ^{13}C NMR study by Heinen et al. [13] on a similar series of polyolefins grafted with ^{13}C-labelled maleic anhydride (MA), which has shown that grafting occurs at CH_2 units of PE and ethene-rich EPMs and at CH units for PP and low-ethene EPMs. The results taken together indicate that selectivity of grafting is determined chiefly by selectivity of H-abstraction.

Machado et al. [15] have studied viscosity changes upon melt processing a similar series of polyolefins in the presence of peroxide. The results establish that for PE and ethene-rich EPMs cross-linking occurs, resulting in increased viscosity, whereas for

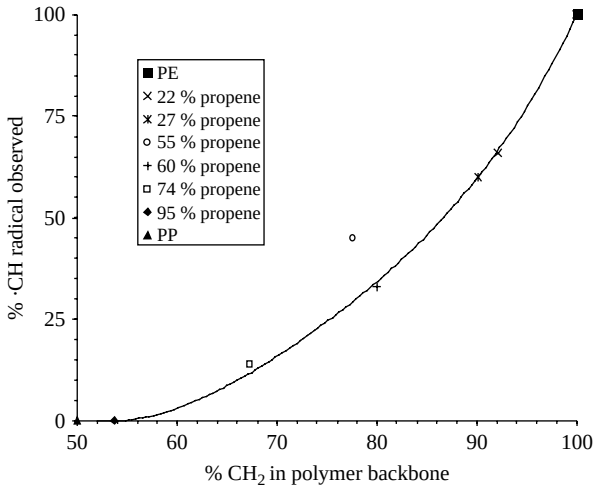

Fig. 8. Plot of percentage secondary radical observed in the EPR spectrum versus the amount of CH_2 present in the EPM polymer backbone.

PP degradation results in reduced viscosity; for EPMs with medium ethene-content, branching and degradation may balance each other leading to as more-or-less constant viscosity. These observations are also consistent with results described here: secondary radicals would be expected to react via combination to give branches and cross-links, whereas, as noted above, tertiary radicals are prone to β-scission (as noted earlier).

Finally, we note that the formation of allyl radicals is, as might be anticipated in terms of results for PE, only observed for those polymers, which contain significant concentrations of –EEE– chains (i.e. random EPM co-polymers with 22, 27 and 55% w/w propene). These findings also reflect, to some extent, the high radical concentration obtained here (as a result of high local radical concentrations) and the enhanced importance of second-order reactions under EPR conditions.

Acknowledgements

We gratefully acknowledge assistance from Jos Aarts, Marcel Aussems and John Mommers (DSM Research) for the analyses of unsaturations using FT-IR spectroscopy, for the studies of oxidation of the model alkenes and alkynes, and for the GC–MS experiments, respectively.

References

[1] Xanthos M. Reactive extrusion, principles and practice. Munich: Hanser Publishers; 1992.
[2] Al-Malaika S, editor. Reactive modifiers for polymers. London: Blackie Academic and Professional; 1997.
[3] Hofman W. Rubber technology. Munich: Hanser Publishers; 1989.
[4] Chodak I, Lazar M. Angew Makromol Chem 1982;106:153.
[5] Chodak I, Fabianova K, Borsig E, Lazar M. Makromol Chem 1978;69: 1073. Chodak I, Zymanyova E. Eur Polym J 1984;20:81.
[6] Borsig E, Fiedlerova A, Lazar M. J Macromol Sci Chem 1981;A16(2):513.
[7] Hamielec AE, Gloor PE, Zhu S. Can J Chem Eng 1991;69:611. Huang C, Duevar T, Tzoganakis C. Polym React Eng 1997;5:1.
[8] Yamazaki T, Seguchi T. J Polym Sci, Part A: Polym Chem 1997;35:279.
[9] Yamazaki T, Seguchi T. J Polym Sci, Part A: Polym Chem 1997;35:2431. Yamazaki T, Seguchi T. J Polym Sci, Part A: Polym Chem 1999;37:349. Yamazaki T, Seguchi T. J Polym Sci, Part A: Polym Chem 2000;38:3092. Yamazaki T, Seguchi T. J Polym Sci, Part A: Polym Chem 2001;39:2151.
[10] Zhou W, Zhu S. Macromolecules 1998;31:4335.
[11] Zhou W, Zhu S. Ind Eng Chem Res 1997;36:1130. Yu Q, Zhu S. Polymer 1999;40:2961.
[12] Yamazaki T, Seguchi T. J Polym Sci, Part A: Polym Chem 2000; 38:3383.
[13] Heinen W, Rosenmoller CH, Wenzel CB, de Groot HJM, Lugtenburg J, van Duin M. Macromolecules 1996;29:1151.
[14] Miyake T, Moriuchi S, Masuda Y, Yamagata F. Nippon Gomu Kyokaishi 1986;59:568.
[15] Machado AV, Covas JA, van Duin M. Polymer 2001;42:3649.
[16] Camara S, Gilbert BC, Meier RJ, van Duin M, Whitwood AC. Org Biomol Chem 2003;1:1181.
[17] Finn M, Friedline R, Suleman NK, Wohl CJ, Tanko JM. J Am Chem Soc 2004;126:7578.
[18] Akzo-Nobel. Initiators for high polymers (peroxide datasheet).
[19] Polymer durability: degradation, stabilization, and lifetime prediction: developed from a symposium sponsored by the Division of Polymer Chemistry, Inc, at the 206th national meeting of the American Chemical Society, Chicago, Illinois, August 22–27, 1993 Clough, RL. (ed); Billingham, NC. (ed); Gillen, KT. (ed); American Chemical Society. Division of Polymer Chemistry. Symposium. Chicago. 1993 Publishers: Washington, ACS Date: 1996 Series: ACS advances in chemistry series no. 249 Classification: 541.64:061.3 LIC Reference Number: 9604.
[20] Bremner T, Rudin A. Plast Rubber Compos Process Appl 1990; 13:61.
[21] Smedburg A, Hjertberg T. Polymer 1997;38:4127.
[22] Hendry DG, Mill T, Pisskiewicz L, Howard JA, Eigenmann HKJ. Phys Chem Ref Data 1974;3(4):937.
[23] Gilbert BC, Trenwith MJ. J Chem Soc, Perkin Trans 2 1973;1834. Kochi JK. Adv Free Radical Chem 1975;5:189.
[24] Gilbert BC, Lindsay Smith JR, Milne EC, Whitwood AC. J Chem Soc, Perkin Trans 2 1994;1759.